

# Density-Functional Theory Calculations of Aqueous Redox Potentials of Fourth-Period Transition Metals

Merle Uudsemaa and Toomas Tamm\*

Department of Chemistry, Tallinn Technical University, Ehitajate tee 5, EE-19086, Estonia

Received: August 4, 2003

Aqueous  $M^{3+}/M^{2+}$  redox potentials for nine of the ten fourth-period transition metals, M, have been calculated with the use of DFT methodology in combination with the COSMO continuum model. Entropy contributions to the potentials are taken from experiments. The model introduces no adjustable parameters beyond those present in the underlying theoretical models. Inclusion of two solvation spheres (18 water molecules) is necessary. For the ions studied, the average absolute difference from experimental values is 0.29 V, with four out of nine potentials (those of V, Cr, Fe, Cu) reproduced with better than 0.1 V accuracy.

## 1. Introduction

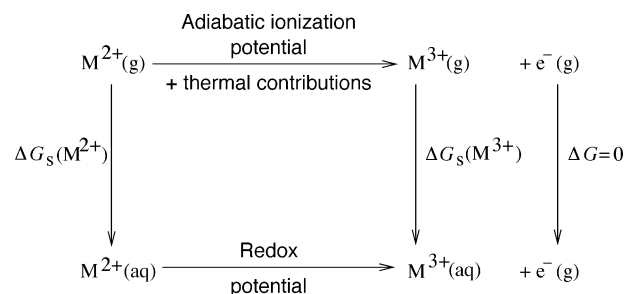
Electrochemistry is one of the few remaining areas of classical chemistry which, until very recently, has been outside the scope of modern quantum-chemical simulations. This can be explained by the complexity of the processes involved in a typical electrochemical reaction. The computing power and sophistication of the underlying models, necessary for an accurate description of electrochemical processes, have become available only in recent years.

Many electrochemical processes occur on the surface of electrodes. Quantum-chemical modeling of such reaction should necessarily take into account the diffusion and adsorption processes on the electrode surface, which leads to considerable system size. From the computational point of view, it would be desirable to avoid modeling of an electrode–solution boundary. This condition is met, for example, in the redox reactions between different oxidation states of transition metal cations in solution.

In the present work, we set a goal of finding a computational approach, based on quantum theory to the largest extent possible, for prediction of aqueous redox potentials of transition metals. We limited ourselves to the elements of the fourth period of the periodic table, mostly to avoid the necessity to account for relativistic effects that will become increasingly prominent in the subsequent periods. We also limited the reactions to  $M^{3+}/M^{2+}$  transitions. For all the elements, Sc–Cu, experimental data for the corresponding potential exist. Zn does not have a stable 3+ cation in aqueous solution, and was therefore not studied in the present work. No true predictions are done in this study. On the other hand, the experimental values were only used to assess the accuracy of the methodology. No parametrization or fitting to experimental data was involved in the production of the proposed model, beyond the parametrization already present in the underlying quantum-chemical methods.

Computational electrochemistry is an emerging field in computational chemistry. Among the pioneering work in this area are the studies of the electrode potential of 2,3-dicyanobenzoquinone by Lister et al.,<sup>1</sup> the calculations by Li et al.<sup>2</sup> on iron and manganese cations, and the use of the semiempirical PM3/SM3 method to model redox potentials of small organic

## SCHEME 1



molecules by Charles-Nicolas and co-workers.<sup>3</sup> More recently, the University of Minnesota research group led by Cramer and Truhlar has published several papers on the subject.<sup>4–6</sup> Baik and Friesner<sup>7</sup> have applied DFT in combination with the SCRf continuum model to a set of redox potentials of organometallic complexes. These studies show that both traditional DFT methods coupled with continuum solvation models, as well as the parametric generalized Born type models are capable of reproducing aqueous redox potentials with 0.1 V or better accuracy. In the case of generalized Born type calculations, the explicit inclusion of water molecules in the model is not needed.

Theoretical calculations of redox potentials typically refer to a free energy cycle. An example of such cycle, adapted for the present systems, is represented in Scheme 1. The free energy change in the redox process (at the bottom of the scheme) is calculated via the gas-phase ionization potential (at the top of the scheme) and the corresponding solvation energies,  $\Delta G_s$ . This approach is discussed in more detail in, e.g., refs 2 and 4.

In the present study we chose to use solvent models of nonparametric type, which do not include fitted parameters beyond van der Waals radii. If such, by their nature less accurate, solvation models are used, it will become necessary to include at least two coordination spheres of water molecules into the model. Quantum-chemical calculations with explicit inclusion of two coordination shells are rare. Li et al.<sup>2</sup> used a model of this type, with partially optimized geometries, to calculate redox potentials and  $pK_a$  values of aqueous manganese and iron cations. Several articles by W. W. Rudolph, C. C. Pye, and co-workers<sup>8–14</sup> have utilized cluster models that include two coordination spheres in the quantum-chemical studies of spectral

\* Corresponding author: E-mail: toomas.tamm@ttu.ee.

**TABLE 1: Experimental Redox Potentials of Fourth-Period Transition Metal Cations in Water**

system	$E^\circ$ , V	original ref	secondary refs
Sc <sup>3+</sup> /Sc <sup>2+</sup>	-2.3	<i>a</i>	[19]
Ti <sup>3+</sup> /Ti <sup>2+</sup>	-0.9	<i>a</i>	[19,20]
	-0.37	[21]	[17,18]
V <sup>3+</sup> /V <sup>2+</sup>	-0.255	[22]	[17,18,19,20]
Cr <sup>3+</sup> /Cr <sup>2+</sup>	-0.41	[23]	[17]
	-0.424	[24]	[18]
	-0.42	[24]	[19]
	-0.407	[23]	[20]
Mn <sup>3+</sup> /Mn <sup>2+</sup>	1.51	[25]	[17]
	1.56	<i>b</i>	[19]
	1.5	[25]	[18]
	1.5415	[26]	[20]
Fe <sup>3+</sup> /Fe <sup>2+</sup>	0.771	[27]	[18,19,20]
Co <sup>3+</sup> /Co <sup>2+</sup>	1.92	[28,29,30]	[18,19,20]
	1.81	[31]	[17]
	1.40–1.53	[32]	-
Ni <sup>3+</sup> /Ni <sup>2+</sup>	2.3	<i>a</i>	[19]
Cu <sup>3+</sup> /Cu <sup>2+</sup>	2.4	<i>a</i>	[19,20]

<sup>a</sup> Values estimated by Bratsch.<sup>19</sup> <sup>b</sup> Value reported by Bratsch,<sup>19</sup> no original reference available.

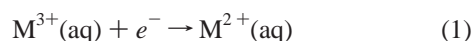
and energetic properties of hydrated cations. A recent paper by the present authors<sup>15</sup> studies the importance of the second coordination sphere in the description of solvation energies of titanium cations.

## 2. Overview of Experimental Data

Several compilations of experimental data on aqueous redox potentials have been published in the past two decades. These include the books by Milazzo et al.,<sup>16</sup> Antelman and Harris,<sup>17</sup> Bard et al.,<sup>18</sup> and the review by Bratsch,<sup>19</sup> as well as several others. The first compilation<sup>16</sup> is spartan in commenting the collected data and, according to its introductory remarks, does not contain any judgment of the quality of the measurements listed. The second one<sup>17</sup> contains almost exclusively numerical data, without references to original research papers. The collection by Bard et al.<sup>18</sup> contains detailed comments on the experimental methods and background of the quoted data. The paper by Bratsch,<sup>19</sup> however, criticizes the latter on the basis of using outdated sources, and contains a lot of data that is missing from the other collections. Many values are marked as “estimated” by the author, without detailed explanations on how these values have been obtained.

We have therefore, for purposes of the present work, tried to trace the necessary reference values to their original sources to the extent possible. Occasionally we have used the CRC Handbook<sup>20</sup> as another source of references. In most cases presented in this work the values listed there are the same as those in the compilation by Bratsch.

We limited ourselves to the transition metals of the fourth period of the periodic table, and to the 3+/2+ transition



as the one that has a corresponding experimental value available for all of the fourth-period *d*-elements except zinc. The available experimental reference data is collected into Table 1. Only the values cited by the compilations (secondary references) are included in this table, alongside the probable primary references.

**Scandium.** Only Bratsch quotes a value for the Sc<sup>3+</sup>/Sc<sup>2+</sup> half-reaction, giving an estimated value of -2.3 V, with a footnote of “this half-reaction involves at least one doubtful chemical species”. This species is obviously Sc<sup>2+</sup>. The accuracy of these estimates is “implied by the number of digits tabulated”,

which we take to mean  $\pm 0.1$  V. No other primary source for a value of this redox potential could be established.

**Titanium.** Bard et al. give a value of -0.368 V for this redox potential, based on the measurements and calculations of Forbes and Hall.<sup>21</sup> Doubt has been cast onto this experiment by later researchers. The compilation also mentions the values -2.1 V<sup>33</sup> and -2.3 V,<sup>34</sup> the latter of which is considered more reliable. Bratsch lists an “estimated” -0.9 V. The implied error bar for this value does not overlap with the ones listed by Bard et al. There is little evidence to support the existence of a stable Ti<sup>2+</sup> cation in aqueous solutions altogether. For the purposes of the present work, we shall use -0.9 V as the “experimental” value, based additionally on the fact that the latest compilations<sup>20</sup> appear to favor it.

**Vanadium.** All sources agree on a value of -0.255 V for V<sup>3+</sup>/V<sup>2+</sup>, with the original work done by G. Jones and J. H. Colvin.<sup>22</sup> Both of the ions involved are stable in acidic solutions.

**Chromium.** Bard et al. list -0.424 V for this redox potential, quoting Grube and Schlechter<sup>24</sup> as the primary (“widely accepted”) reference. Alternatives, discussed in the text, are -0.422 V,<sup>24</sup> -0.4295 V,<sup>35</sup> and -0.402 V.<sup>23</sup> Bratsch uses a more cautious -0.42 V, implying larger error bars. The recent CRC Handbook, however, lists -0.407 V for the Cr<sup>3+</sup>/Cr<sup>2+</sup> pair, which might be derived from the -0.402 V of ref 23. In the present work, we shall use -0.42 V as a compromise.

**Manganese.** Here, Bratsch has a value with three significant digits, 1.56 V, while Bard et al. have a more cautious 1.5 V, based on two sources.<sup>25,26</sup> The very accurate 1.5415 V in the CRC Handbook is the result of a measurement by Ciavatta and Grimaldi.<sup>26</sup> While Bard et al. quote this source, they exercise caution about the accuracy of this measurement. We shall adopt the value of 1.54 V for this study, which is supported by the latest and apparently most accurate measurement, and is close to the average of all available values.

**Iron.** All sources agree on +0.771 V for Fe<sup>3+</sup>/Fe<sup>2+</sup>, based on at least two measurements.<sup>27,36</sup>

**Cobalt.** All compilations also agree on the Co<sup>3+</sup>/Co<sup>2+</sup> redox potential, which has the value of +1.92 V. However, several measurements exist which disagree with this value. In chronological order, the published values are 1.92 V,<sup>28</sup> 1.93 V,<sup>37</sup> 1.92 V,<sup>29</sup> 1.81 V,<sup>31</sup> 1.82–1.86 V,<sup>30</sup> 1.45 V.<sup>32</sup> Experimental measurements are complicated due to the oxidation of water by the Co<sup>3+</sup> cation,<sup>18</sup> and by dimerization of the Co<sup>3+</sup> ions in aqueous solution.<sup>30</sup> We shall adopt 1.92 V as the reference value here, but will keep in mind that the actual value of the potential may be lower, as indicated by the more recent measurements.

**Nickel.** Only Bratsch lists an “estimated” value of +2.3 V for the Ni<sup>3+</sup>/Ni<sup>2+</sup> redox couple.

**Copper.** Again, the only available value for the Cu<sup>3+</sup>/Cu<sup>2+</sup> redox potential is one estimated by Bratsch, +2.4 V.

**Zinc.** The Zn<sup>3+</sup> cation is unknown in aqueous solutions and the corresponding redox potentials have not been established. We did not carry out any calculations for zinc complexes in the present work.

In conclusion, two out of the nine experimental potentials (Ti<sup>3+</sup>/Ti<sup>2+</sup>, Co<sup>3+</sup>/Co<sup>2+</sup>) have significant experimental uncertainties. For these, several competing values exist, with nonoverlapping error bars. Several of the other redox potentials in the list involve at least one suspicious or unstable chemical species, or have a single, “estimated” value and may thus also contain experimental errors.

Nevertheless, we covered all of the listed electrochemical couples, except that of zinc, in the present study, with the intent to establish the applicability of DFT methodology in combina-

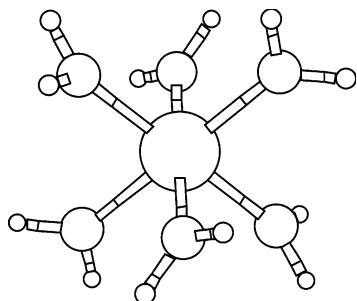


Figure 1. Six-water model cation complex.

tion with a continuum solvation model for reproduction of aqueous redox potentials.

### 3. Model Geometries

The most simplistic quantum-chemical model for a solvated metal ion in water would include the bare ion alone, embedded in a dielectric continuum. The energy of solvation  $E_{\text{solv}}$  (and, consequently, calculated redox potentials) for spherical ions are dominated by the Born term<sup>38</sup>

$$E_{\text{solv}} = \frac{1 - \epsilon}{\epsilon a_0} Q^2 \quad (2)$$

where  $\epsilon$  is the dielectric constant of the solvent,  $a_0$  is the radius of the cavity in the solvent accommodating the ion, and  $Q$  is the ionic charge.

The Born term for a spherical charged species is relatively large compared to the similar dipolar, quadrupolar, etc. terms for electroneutral polar molecules. Other terms contributing to the energy of solvation, such as those due to cavitation and dispersion, are smaller in absolute values and thus of lesser importance in determining the accuracy of energetic estimates. In principle, it is possible to adjust the cavity radius,  $a_0$ , to fit the experimental data. This type of fitting was not pursued in the present work.

Available experimental evidence<sup>39</sup> suggests that the ions of fourth-period transition metals are hexacoordinated in water. This naturally leads to a model which includes the first solvation sphere (ligands) in the quantum-mechanical part of the calculation, possibly surrounded by a continuum model to account for the nonspecific solvation effects. The water molecules are assumed to be oriented with oxygen atoms toward the central, positively charged, ion. This type of model shall be subsequently called the “six-water” model (Figure 1). Such models have been widely employed in studies of hydrated ionic complexes. In the present calculations, octahedral symmetries were originally assumed, but symmetry breaking was allowed during geometry optimization. Furthermore, asymmetric starting geometries were employed in order to avoid high-symmetry local minima where lower-energy, lower-symmetry ones might be separated from the former by small barriers.

The model can be expanded by adding a second coordination sphere to it. In this work this was done by attaching a hydrogen-bonded water molecule to each hydrogen atom of the first sphere, thus yielding the “18-water” model. In an idealized form, such model has  $T_h$  symmetry and has been used earlier<sup>2</sup> (Figure 2). The authors of the cited work acknowledged that they had not necessarily reached a minimum on the potential energy surface. In other studies,<sup>9–14</sup> related local minima with  $T$  symmetry were found for the  $M(\text{OH}_2)_{18}^{2+}$  ( $M = \text{Li, Mg, Sc, Cd, Al}$ ) systems. Our own test calculations confirmed that for several ions considered here, this conformation is not a

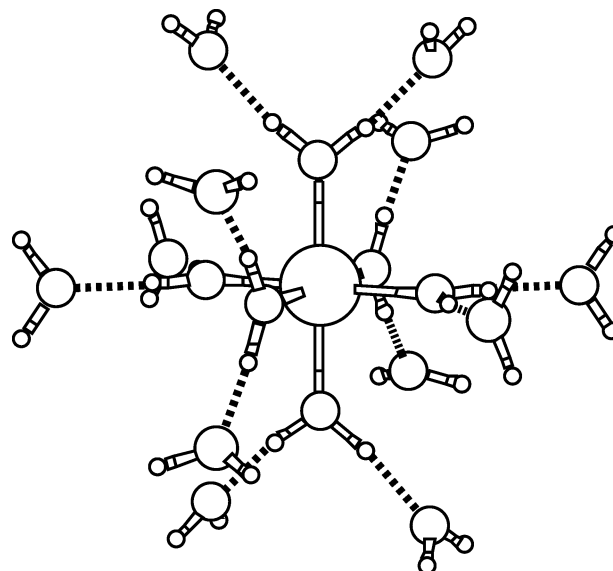


Figure 2. 18-Water model cation complex with  $T_h$  symmetry.

minimum, but a high-order transition state.<sup>15</sup> Full geometry optimizations of the model systems were therefore carried out. The various minima obtained are described subsequently.

### 4. Computational Method

Density-functional theory (DFT) calculations were performed using the Becke–Perdew ‘86 (BP86) exchange and correlation functionals. This choice of functional was dictated by it being of the nonhybrid variety. Application of hybrid functionals (B3LYP in particular) to transition metal systems has recently been criticized.<sup>40,41</sup> Also, use of a nonhybrid functional allowed the use of “resolution of identity”<sup>42</sup> (RI) approximation in the calculations, which leads to considerable savings of CPU time.

Geometries of the systems were optimized within the RI approximation, using the SV(P) basis set of Ahlrichs et al.<sup>43</sup> The geometries of the 18-water systems thus obtained were used for calculation of vibrational frequencies at the BP86/SV(P) level, leading to the zero-point vibrational contribution to the total energy (ZPE). Lack of imaginary eigenvalues of the Hessian was also used to confirm the stationary points as true minima on the potential energy surface.

The optimization was continued from the SV(P) geometry with the use of the TZVPP basis set<sup>44</sup> and the RI approximation for the 18-water systems. Since only small changes in geometries were observed during this optimization, it was assumed that the validation of minima at SV(P) level was sufficient and no further vibrational calculations were performed for the 18-water model systems. The 6-water systems, however, easily yielded to full optimization and vibrational analysis at the BP86/TZVPP level without using the RI approximation, and were characterized at this level of theory.

At the final TZVPP geometry, a single-point calculation was performed without using the RI approximation. This would yield the final electronic energy of the system of the 18-water models.

The remaining (bulk) solvent was modeled with the COSMO<sup>45</sup> continuum model. No changes were made into the default cavity radii used by the Turbomole software. The “optimized” atomic radii of oxygen (1.72 Å) and hydrogen (1.30 Å), as defined in the Turbomole program, were used for construction of the cavity in the solvent. No optimized values were available for the transition metals, and the Bondi<sup>46</sup> values were used for them. Very little, if any, of the central ion surface

**TABLE 2: Calculated Redox Potentials, Using Eqs 3–4, in Volts**

system	ion	ion + contin.	ion + 6 H <sub>2</sub> O	ion + 6 H <sub>2</sub> O + contin.	ion + 18 H <sub>2</sub> O	ion + 18 H <sub>2</sub> O + contin.	expt.
Sc <sup>3+</sup> /Sc <sup>2+</sup>	21.77	5.88	9.24	-0.75	5.16	-1.61	-2.3
Ti <sup>3+</sup> /Ti <sup>2+</sup>	24.67	8.80	10.20	0.09	6.07	-0.75	-0.9
V <sup>3+</sup> /V <sup>2+</sup>	26.02	10.33	11.23	1.00	6.63	-0.17	-0.255
Cr <sup>3+</sup> /Cr <sup>2+</sup>	27.09	11.19	11.09	0.72	6.41	-0.50	-0.42
Mn <sup>3+</sup> /Mn <sup>2+</sup>	30.06	14.15	13.06	2.70	8.07	1.21	1.54
Fe <sup>3+</sup> /Fe <sup>2+</sup>	27.89	11.98	12.08	1.92	7.55	0.73	0.77
Co <sup>3+</sup> /Co <sup>2+</sup>							
Co <sup>3+</sup> Mult=1	34.19	18.27	13.28	2.50	8.09	1.10	1.92
Co <sup>3+</sup> Mult=5	30.62	14.70	13.24	3.09	8.53	1.75	1.92
Ni <sup>3+</sup> /Ni <sup>2+</sup>							
Ni <sup>3+</sup> Mult=2	33.48	17.40	14.11	3.58	8.84	1.94	2.3
Ni <sup>3+</sup> Mult=4	31.96	16.04	14.05	3.97	9.11	2.24	2.3
Cu <sup>3+</sup> /Cu <sup>2+</sup>	33.27	17.36	13.89	3.66	9.22	2.32	2.4

**TABLE 3: Differences between Calculated and Experimental Redox Potentials, in Volts**

system	ion	ion + contin.	ion + 6 H <sub>2</sub> O	ion + 6 H <sub>2</sub> O + contin.	ion + 18 H <sub>2</sub> O	ion + 18 H <sub>2</sub> O + contin.
Sc <sup>3+</sup> /Sc <sup>2+</sup>	24.07	8.18	11.54	1.55	7.46	0.69
Ti <sup>3+</sup> /Ti <sup>2+</sup>	25.57	9.70	11.10	0.99	6.97	0.15
V <sup>3+</sup> /V <sup>2+</sup>	26.28	10.58	11.49	1.26	6.89	0.08
Cr <sup>3+</sup> /Cr <sup>2+</sup>	27.51	11.61	11.51	1.14	6.83	-0.08
Mn <sup>3+</sup> /Mn <sup>2+</sup>	28.52	12.61	11.52	1.16	6.53	-0.33
Fe <sup>3+</sup> /Fe <sup>2+</sup>	27.12	11.21	11.31	1.15	6.78	-0.04
Co <sup>3+</sup> /Co <sup>2+</sup>						
Co <sup>3+</sup> Mult=1	32.27	16.35	11.36	0.58	6.17	-0.82
Co <sup>3+</sup> Mult=5	28.70	12.78	11.32	1.17	6.61	-0.17
Ni <sup>3+</sup> /Ni <sup>2+</sup>						
Ni <sup>3+</sup> Mult=2	31.18	15.10	11.81	1.28	6.54	-0.36
Ni <sup>3+</sup> Mult=4	29.66	13.74	11.75	1.67	6.81	-0.06
Cu <sup>3+</sup> /Cu <sup>2+</sup>	30.87	14.96	11.49	1.26	6.82	-0.08

is exposed to the bulk solvent, therefore the accuracy of these radii is expected not to be critical.

All calculations were performed with the Turbomole,<sup>47</sup> version 5.5, program package. The basis sets, density functional, and the COSMO model were used as defined in this code.

## 5. Results and Discussion

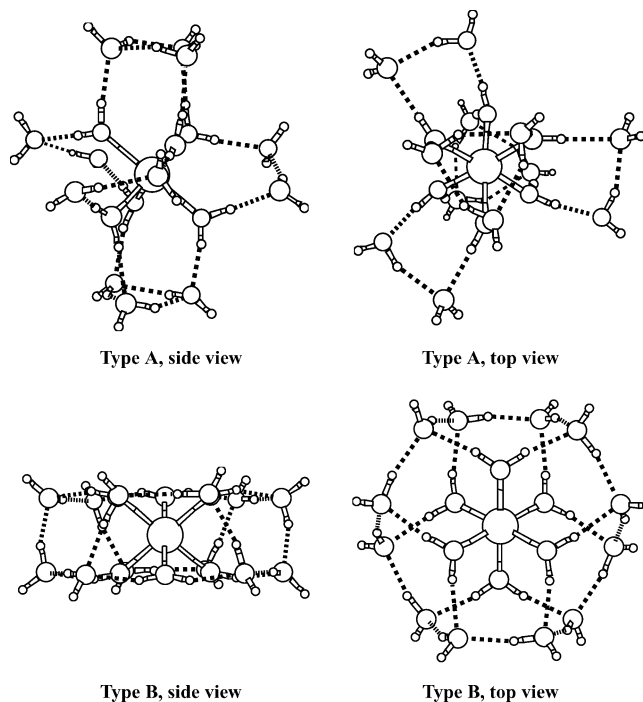
The main numerical results are collected into Tables 2 and 3. Final optimized geometries, total energies in Hartree units, and the components of redox potentials (IPs, solvation energies, etc.) are available in the electronic Supporting Information.

**Geometries.** When only the first solvation shell (ligands) of the ions was modeled, local minima of several symmetry groups were located. The symmetries are in good agreement with results of earlier similar studies.<sup>48,49</sup>

With the second coordination sphere included in the model, several local minima were located for several of the ions. Examples of some of the typical minimum geometries are found in Figure 3. The types of minima (A and B) are discussed in more detail in our earlier work.<sup>15</sup> A geometry similar to our Type B has also recently been reported for Mg(OH<sub>2</sub>)<sub>18</sub><sup>2+</sup> by G. D. Markham et al.<sup>50</sup>

Relative energies of clusters with both types of minima were calculated for the titanium and vanadium ions. Type B turned out to be energetically more favorable for three out of four test cases (Ti<sup>2+</sup>, V<sup>2+</sup>, V<sup>3+</sup>). Even for the Ti<sup>3+</sup>, where type A had lower energy, the energetic difference between the two types of clusters was small (8 kJ/mol with ZPE included). A large change in the geometry of the water cluster in the redox process is unlikely. No low-barrier path between the two minima was established. Therefore, we chose to use a type B geometry in all the 18-water calculations. The geometry was reoptimized for each individual ion.

The geometry of the first solvation sphere (ligands) is significantly affected by the presence of the second solvation

**Figure 3.** Optimized geometries for the 18-water models.

sphere in the model. The typical arrangement of the ligand water molecules in type B complexes, with the outer solvation sphere removed, has near-*D*<sub>3d</sub> symmetry (Figure 4), the water molecules turned “horizontal”. The gas-phase geometries of six-ligand ion–water clusters are not characteristic of the same ions in the presence of additional water layers.

As explained above, the geometries of the 18-water clusters were optimized with both SV(P) and TZVPP basis sets. The former does not possess polarization functions on the hydrogen atoms. This has its influence on the geometries of the hydrogen

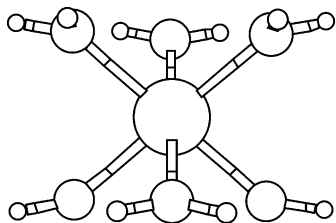


**Figure 4.** The first coordination sphere of  $V^{2+}$  in the 18-water model with the outer 12 water molecules not shown.

bonds between the water molecules. The following examples are for the  $Fe(OH_2)_{18}^{3+}$  cluster. The hydrogen bond length between the inner and outer coordination sphere is relatively insensitive to the change in basis set, with typical values of 163–166 pm using SV(P) and 168–170 for TZVPP, the average increase in length being 4 pm. The hydrogen bonds between the molecules in the outer coordination sphere are more sensitive, with an average increase of 23 pm, from around 168 pm to 191 pm. The overall topology of the hydrogen bond network does not change with the change in the basis set, however.

**Redox Potentials.** Redox potentials of the ions in aqueous solution were calculated from the thermodynamic cycle represented in Scheme 1, which leads to the following equation:<sup>2</sup>

$$E_{\text{redox}} = IP(g) - \Delta\Delta E_{\text{sol}} + T\Delta S + \Delta E_{\text{SHE}} \quad (3)$$

where  $IP(g)$  is the computed ionization potential of the corresponding ion–water cluster, calculated as the difference of energies for the optimized geometries of the corresponding cation complexes. Difference between the corresponding zero-point vibrational energies was also added into this term. The  $\Delta\Delta E_{\text{sol}}$  term is the difference in continuum solvation energies of the ion–water clusters, calculated in a single-point COSMO calculation for the participating systems. Cavitation and dispersion terms were not calculated, since the size and shape of the cavity does not change significantly between the two differently charged states of a given ion.

The entropy term  $T\Delta S$  is the only component of  $E_{\text{redox}}$  that we were unable to calculate using a theoretical approach. Attempts were made to make use of vibrational and rotational entropies of the clusters, but the resulting  $\Delta S$  values turned out about an order of magnitude smaller than the experimental ones. For example, the rovibrational entropy of the  $Fe(OH_2)_{18}^{3+}$  was calculated as 0.84248 kJ/(mol·K), that of  $Fe(OH_2)_{18}^{2+}$  as 0.85564 kJ/(mol·K), with the difference being 0.01316 kJ/(mol·K). The corresponding experimental difference for the  $Fe^+/Fe^{2+}$  redox pair is 1.175 mV/K = 0.1134 kJ/(mol·K), however. A similar difference is found for the six-water clusters, thus we suspect that the origin of the difference lies in the description of the ion–ligand bonds.

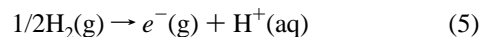
We therefore used the temperature dependency data from the compilation by Bratsch,<sup>19</sup> which yielded  $\Delta S$  as

$$\Delta S_{298}^{\circ} = nF(dE^{\circ}/dT)_{298} \quad (4)$$

where  $F$  is the Faraday constant and  $n$ , number of electrons transferred (1 in the present study). The standard temperature of 298 K was used in eq 3. The entropy data were used “as is”, without additional fitting for the purposes of the present model.

Due to use of different standard states in quantum chemistry and electrochemistry (see the Appendix in ref 5 for an excellent discussion), a term correcting for this difference,  $\Delta E_{\text{SHE}}$ , needs to be included. This term corresponds to the absolute potential

for the reference electrode process



in a vacuum, and was taken to be 4.43 eV.<sup>51</sup> This is an experimental value, which, again, was not adjusted for the purposes of this study.

**Comparison of Models.** As the data in Tables 2 and 3 indicate, the gas-phase adiabatic ionization potential is a very poor approximation to aqueous redox potential. Differences from the experimental values are typically 20–30 V. This can be expected since all the relaxation effects in the solvent are neglected in this approximation, leading to a gross overestimation of the energy difference between the two oxidation states in the aqueous environment.

Introduction of a continuum solvation model (COSMO), which for spherical ions includes primarily the Born term, does not improve the quality of predictions significantly. Differences from experiment remain high, being 10–15 V for most cases. Use of default atomic radii and neglect of cavitation and dispersion terms are the main contributing factors to this failure.

It should be noted, however, that for larger molecules, more advanced semiempirical solvation models such as SM5.42R<sup>52</sup> are capable of significantly better accuracy in reproduction of aqueous redox potentials.<sup>4,5</sup>

Surrounding of the central ion by one or two explicit solvation shells is thus essential for obtaining better accuracy. The first solvation shell (ligands, six water molecules in our model) alone does not improve the differences from experiment beyond those obtained by using a continuum model alone. It is significant, however, that the differences are almost constant, ranging from 11.10 to 11.81 V. Based on the present limited selection of ions, use of the adiabatic ionization potential of a hexa-aqua complex in gas phase could be used as an estimate for the aqueous redox potential, if a correction of 11.46 V (average for the ions in this study) is added.

Surrounding of the six-ligand model with a dielectric continuum brings the redox potentials into the experimental range. The values remain typically about 1–1.6 V too positive, with cobalt as an exception with even smaller difference.

Use of two explicitly modeled solvation spheres (18 water molecules) also reduces the difference between calculated and experimental values. The reduction is not dramatic when compared to the six-water model: the differences drop from 11.46 to an average of 6.78 V. While the inclusion of the explicit second solvation sphere almost halves the gap between the calculation and experiment, it is clearly not sufficient alone to bring the results nearly as close to experimental values as the continuum model does.

When the second coordination sphere is combined with a continuum model, however, the resulting calculated redox potentials approach experimental accuracy. Differences from the experiment are less than 0.5 V in most cases, and better than 0.1 V for four of the systems (vanadium, chromium, iron, copper).

It would be of interest to know whether the results have converged with respect to cluster size. Unfortunately, addition of a third solvation layer would be too demanding computationally and was thus not pursued in the present study. If introduced, the additional layer should be modeled quantum-chemically, since charge transfer is expected between the layers. As we have reported previously,<sup>15</sup> and also observed in the course of this work, charge transfer between solvation layers is significant. Therefore, combined quantum mechanical/molecular mechanical models were not used in this study either.

Inclusion of a continuum model appears to be significant in all cases explored so far. Given the charged nature of the system, the difference between Born terms (eq 2) remains an essential contributor to the energy difference between the systems having 2+ and 3+ charge. With the term being inversely proportional to the cavity size, the difference is expected to remain significant even with much larger cavities (e.g., the hypothetical case of explicitly modeling several additional layers of water molecules).

The average absolute difference from experiment across the nine redox potentials is 0.29 V. In the next section it will be shown that for two systems,  $\text{Co}^{3+}/\text{Co}^{2+}$  and  $\text{Ni}^{3+}/\text{Ni}^{2+}$ , better results are obtained if an open-shell electronic structure is assumed for the trivalent state. When such adjustment is made, the average absolute difference drops to 0.19 V.

For most of the ions in this study, the combined 18-water plus continuum model errs toward the negative side of the experimental values. All the simpler models had differences from the experimental values in the positive direction. It cannot be excluded that a cancellation of errors is taking place here. Whether inclusion of further coordination spheres or, perhaps, time-averaged dynamics, would further improve the results are topics for further studies.

**Performance of Models for the Specific Ions.** *Scandium.* None of the models used here gives a good value for the  $\text{Sc}^{3+}/\text{Sc}^{2+}$  redox potential. Differences between experimental and calculated values remain larger than 0.69 V. This is the second largest difference in the present series. In view of the fact that the 18-water + continuum model performs well for many of the other redox potentials, and the admittance by Bratsch<sup>19</sup> that the experimental value is estimated and contains a doubtful chemical species, one cannot exclude that the large difference may be due to experimental error, rather than inadequacy of the present model.

*Titanium.* The calculated value for the redox potential,  $-0.75$  V, is off by 0.15 V of the value  $-0.9$  V estimated by Bratsch. We consider this a good result, given the high uncertainty of the experimental data with estimates ranging from  $-0.37$  V to  $-2.3$  V.

*Vanadium.* The experimentally well-established  $\text{V}^{3+}/\text{V}^{2+}$  redox potential at  $-0.255$  V is well reproduced by the best model in the present work, giving a value of  $-0.17$  V, which is 0.08 V more positive than the experimental one.

*Chromium.* Despite the uncertainty of the second and subsequent significant digits of the experimental  $\text{Cr}^{3+}/\text{Cr}^{2+}$  redox potential, all the known experimental values are within 0.1 V of the  $-0.50$  V calculated here. While the differences from experiment were positive for the three prior redox pairs, our model gives a negative difference for chromium, as well as all the subsequent ions.

*Manganese.* The performance of the 18-water + continuum model is not as good for  $\text{Mn}^{3+}/\text{Mn}^{2+}$  as it is for the two previous, as well as the next, ion. Even though experimental results with up to five significant digits have been published, other authors<sup>18</sup> dare not to go beyond a cautious "about 1.5 V" for this value. Even so, the difference between calculated and experimental value remains unsatisfyingly high here, 0.3–0.4 V when different experiments are used for comparison.

*Iron.* The experimentally thoroughly researched  $\text{Fe}^{3+}/\text{Fe}^{2+}$  potential at  $-0.77$  V is reproduced with only  $-0.04$  V difference in the present work. It is reassuring to know that the model performs well for this practically important and much-researched redox couple.

*Cobalt.* Use of the standard 18-water + continuum model for the  $\text{Co}^{3+}/\text{Co}^{2+}$  system leads to a significant discrepancy with

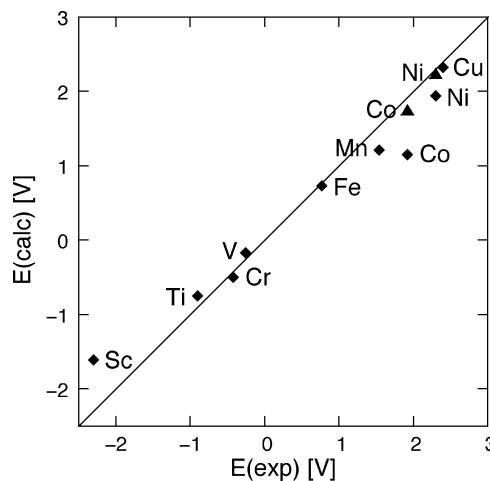


**Figure 5.** Experimental and calculated redox potentials. The calculated values correspond to the 18-water + continuum model. Triangles indicate the calculations which involve high-spin trivalent Co and Ni cations.

the experimental value:  $-0.82$  V. Even though it is experimentally known that the  $\text{Co}^{3+}$  ion is low-spin in the solution, and the low-spin species also has lower energy in the present calculations (by a margin of 0.44 eV, or 42 kJ/mol), it turned out that use of the energy of a high-spin  $\text{Co}^{3+}$  would lead to a value of redox potential that is much closer to the accepted experimental value, leaving only a  $-0.17$  V gap between experiment and calculation.

It has been reported,<sup>30</sup> that the  $\text{Co}^{3+}$  ion dimerizes in the aqueous solution to a significant extent.  $\text{Co}^{3+}$  also oxidizes water.<sup>18</sup> Therefore the concentration of monomeric  $\text{Co}^{3+}$  cannot be well established in the experiments. It cannot be excluded that the experimental values reported for  $\text{Co}^{3+}/\text{Co}^{2+}$  are biased due to this effect.

As reviewed earlier, there are several reported experimental values for the  $\text{Co}^{3+}/\text{Co}^{2+}$  available in the literature. The one that is most widely accepted, 1.92 V, and used in the present work as reference, is the one most removed from the calculated value of 1.15 V (assuming low-spin  $\text{Co}^{3+}$ ). Should any of the values from later experiments, which vary from 1.45 to 1.93 V, be more widely adopted, the difference between calculation and experiment would correspondingly be reduced.

*Nickel.* Just as with the case of cobalt, use of the higher multiplicity for  $\text{Ni}^{3+}$  in the calculation leads to a redox potential closer to experiment. The difference is  $-0.36$  V for the low-spin (experimentally observed) case and  $-0.06$  V for the high-spin  $\text{Ni}^{3+}$ . Additionally, there is very limited experimental evidence to support the  $+2.3$  V redox potential estimated by Bratsch.

*Copper.* Here, the model yields a value reasonably close to the experimental one (difference  $-0.1$  V). The experimental value itself, again contains a doubtful chemical species ( $\text{Cu}^{3+}$ ) and is a mere estimate. Thus it is hard to tell whether we are observing anything more than a coincidence here.

**Summary.** The 18-water + continuum model appears to work well for the systems where the experimental values are well established. The less accurate results coincide with the cases where there have been experimental difficulties in establishing a reliable redox potential.

One possible cause for the discrepancies in the cases of  $\text{Ni}^{3+}/\text{Ni}^{2+}$  and  $\text{Co}^{3+}/\text{Co}^{2+}$  can lie in the entropy contributions that arise from change of spin-state of the central ion. The effects can be as large as 0.25 V, depending on the spin-state of either the  $\text{M}^{3+}$  or  $\text{M}^{2+}$  complex. This stems from the change in the

nature of chemical bond between the central ion and the ligands, which in turn changes the vibrational contributions to the entropy.<sup>53,54</sup> Because the vibrational entropy was not modeled in the course of the present work, we were unable to assess the importance of this phenomenon to the accuracy of the results obtained.

Figure 5 summarizes the experimental and calculated redox potentials. While the correlation is far from perfect, the model obviously works for a wide range (in terms of values in volts) of redox potentials.

Table 3 lists the average absolute errors for the different models studied in the present work. Once more, the significance of combining two coordination spheres and a continuum model is evident.

## 6. Conclusion

As the present work shows, current DFT and continuum solvation models, when combined with explicitly modeled solvent molecules, are capable of reproducing experimental redox potentials with an average error of 0.29 V. The only empirical electrochemical parameter in the model is the entropy contribution to the redox potential, which could not be estimated reliably at the present level of theory. In the preparation of this model, we did not introduce any additional adjustable parameters.

For two of the species studied,  $\text{Co}^{3+}$  and  $\text{Ni}^{3+}$ , better results are obtained if a high-spin species is included in the calculation, despite experimental evidence that the low-spin ion is the dominant form in the solution. Other explanations for this discrepancy, such as dimerization,<sup>30</sup> are also possible.

**Acknowledgment.** This work was supported by Estonian Science Foundation grant no. 3663 and the Ministry of Education of Estonia. We also acknowledge the remarks of the anonymous referees of a previous version of this paper which pointed us to several important literature references and led to numerous improvements in the manuscript.

**Supporting Information Available:** Cartesian coordinates (in Bohr units) of the minima of the 6-water and 18-water model systems that were used for calculation of redox potentials; components (IP,  $E_{\text{sol}}$ ,  $T\Delta S$ ) used for calculation of redox potentials; calculated energies (in Hartrees, BP86/TZVPP) of the systems. This material is available free of charge via the Internet at <http://pubs.acs.org>.

## References and Notes

- Lister, S. G.; Reynolds, C. A.; Richards, W. G. *Int. J. Quantum Chem.* **1992**, *41*, 293–310.
- Li, J.; Fisher, C. L.; Chen, J.; Bashford, D.; Noodleman, L. *Inorg. Chem.* **1996**, *35*, 4694–4702.
- Charles-Nicolas, O.; Lacroix, J. C.; Lacaze, P. C. *J. Chim. Phys.* **1998**, *95*, 1457–1460.
- Winget, P.; Weber, E. J.; Cramer, C. J.; Truhlar, D. G. *Phys. Chem. Chem. Phys.* **2000**, *2*, 1231–1239.
- Patterson, E. V.; Cramer, C. J.; Truhlar, D. G. *J. Am. Chem. Soc.* **2001**, *123*, 2025–2031.
- Arnold, W. A.; Winget, P.; Cramer, C. J. *Environ. Sci. Technol.* **2002**, *36*, 3536–3541.
- Baik, M.-H.; Friesner, R. A. *J. Phys. Chem. A* **2002**, *106*, 7407–7412.
- Pye, C. C.; Rudolph, W.; Poirier, R. A. *J. Phys. Chem.* **1996**, *100*, 601–605.
- Rudolph, W. W.; Pye, C. C. *J. Phys. Chem. B* **1998**, *102*, 3564–3573.
- Pye, C. C.; Rudolph, W. W. *J. Phys. Chem. A* **1998**, *102*, 9933–9943.
- Rudolph, W. W.; Pye, C. C. *Phys. Chem. Chem. Phys.* **1999**, pp 4583–4593.
- Rudolph, W. W.; Mason, R.; Pye, C. C. *Phys. Chem. Chem. Phys.* **2000**, pp 5030–5040.
- Pye, C. C. *Int. J. Quantum Chem.* **2000**, *76*, 62–76.
- Rudolph, W. W.; Pye, C. C. *J. Phys. Chem. A* **2000**, *104*, 1627–1639.
- Uudsemaa, M.; Tamm, T. *Chem. Phys. Lett.* **2001**, *342*, 667–672.
- Milazzo, G.; Caroli, S.; Sharma, V. K. *Tables of standard electrode potentials*; Wiley-Interscience: Chichester, 1978.
- Antelman, M. S.; Harris, F. J. *The Encyclopedia of Chemical Electrode Potentials*; Plenum: London, 1982.
- Bard, A. J.; Parsons, R.; Jordan, J. *Standard potentials in aqueous solution*; Marcel Dekker: New York, 1985.
- Bratsch, S. G. *J. Phys. Chem. Ref. Data* **1989**, *18*, 1–21.
- Lide, D. R. *CRC Handbook of Chemistry and Physics*; CRC Press: Boca Raton, 2002.
- Forbes, G. S.; Hall, I. P. *J. Am. Chem. Soc.* **1924**, *46*, 385–390.
- Jones, G.; Colvin, J. H. *J. Am. Chem. Soc.* **1944**, *66*, 1563–1571.
- Forbes, G. S.; Richter, W. H. *J. Am. Chem. Soc.* **1917**, *39*, 1140–1148.
- von Grube, G.; Schlecht, L. Z. *Electrochem.* **1926**, *32*, 178–186.
- Vetter, K. J.; Manecke, G. Z. *Phys. Chem.* **1950**, *195*, 270–280.
- Ciavatta, L.; Grimaldi, M. J. *Inorg. Nucl. Chem.* **1969**, *31*, 3071–3082.
- Schumb, W. C.; Sherrill, M. S.; Sweetser, S. B. *J. Am. Chem. Soc.* **1937**, *59*, 2360–2365.
- Diebler, H.; Sutin, N. *J. Phys. Chem.* **1964**, *68*, 174–180.
- Huchital, D. H.; Sutin, N.; Warnqvist, B. *Inorg. Chem.* **1967**, *6*, 838–840.
- Warnqvist, B. *Inorg. Chem.* **1970**, *9*, 682–684.
- Rock, P. A. *Inorg. Chem.* **1968**, *7*, 837–840.
- Rotinjan, A. L.; Borisowa, L. M.; Boldin, R. W. *Electrochim. Acta* **1974**, *19*, 43–46.
- Olver, J. W.; Ross, J. W. *J. Am. Chem. Soc.* **1963**, *85*, 2565–2566.
- George, P.; McClure, D. S. *Progress in inorganic chemistry*; Interscience: New York, 1959; Vol. 1.
- Biedermann, G.; Romano, V. *Acta Chem. Scand. A* **1975**, *29*, 615–622.
- Whittemore, D. O.; Langmuir, D. J. *Chem. Eng. Data* **1972**, *17*, 288–290.
- Johnson, D. A.; Sharpe, A. G. *J. Chem. Soc.* **1964**, pp 3490–3492.
- Born, M. Z. *Physik.* **1920**, *1*, 45–48.
- Greenwood, N. N.; Earnshaw, A. *Chemistry of the Elements*; Butterworth-Heinemann: Oxford, 1997.
- Sellmann, D.; Gottschalk-Gauding, T.; Häussinger, D.; Heinemann, F. W.; Hess, B. A. *Chem. Eur. J.* **2001**, *7*, 2099–2103.
- Sellmann, D.; Blum, N.; Heinemann, F. W.; Hess, B. A. *Chem. Eur. J.* **2001**, *7*, 1874–1880.
- Eichkorn, K.; Weigend, F.; Treutler, O.; Ahlrichs, R. *Theor. Chim. Acta*, **1997**, *97*, 119–124.
- Schäfer, A.; Horn, H.; Ahlrichs, R. *J. Chem. Phys.* **1992**, *97*, 2571–2577.
- Schäfer, A.; Huber, C.; Ahlrichs, R. *J. Chem. Phys.* **1994**, *100*, 5829–5835.
- Klamt, A.; Schüürmann, G. *J. Chem. Soc., Perkin Trans. 2.* **1993**, pp 799–805.
- Bondi, A. *J. Phys. Chem.* **1964**, *68*, 441–451.
- Ahlrichs, R.; Bär, M.; Häser, M.; Horn, H.; Kölmel, C. *Chem. Phys. Lett.* **1989**, *162*, 165–169.
- Tachikawa, H.; Ichikawa, T.; Yoshida, H. *J. Am. Chem. Soc.* **1990**, *112*, 982–987.
- Hartmann, M.; Clark, T.; van Eldik, R. *J. Phys. Chem. A* **1999**, *103*, 9899–9905.
- Markham, G. D.; Glusker, J. P.; Bock, C. W. *J. Phys. Chem. B* **2002**, *106*, 5118–5134.
- Reiss, H.; Heller, A. *J. Phys. Chem.* **1985**, *89*, 4207–4213.
- Zhu, T.; Li, J.; Hawkins, G. D.; Cramer, C. J.; Truhlar, D. G. *J. Chem. Phys.* **1998**, *109*, 9117–9133.
- Richardson, D. E.; Sharpe, P. *Inorg. Chem.* **1991**, *30*, 1412–1414.
- Turner, J. W.; Schultz, F. A. *Inorg. Chem.* **1999**, *38*, 358–364.